

Current Biology

Single-Neuron Correlates of Conscious Perception in the Human Medial Temporal Lobe

Highlights

- Neurons fire in response to their preferred stimulus also in absence of awareness
- Neuronal responses to unseen versus seen stimuli are delayed and more dispersed
- Firing rates to seen versus unseen stimuli are increased
- These correlates of awareness are strongest in anterior regions of the MTL

Authors

Thomas P. Reber, Jennifer Faber, Johannes Niediek, Jan Boström, Christian E. Elger, Florian Mormann

Correspondence

florian.mormann@ukbonn.de

In Brief

Reber et al. demonstrate that neurons in the human MTL also fire in response to unseen visual stimuli and that not only strength but also timing of neuronal responses indicates conscious perception.

Single-Neuron Correlates of Conscious Perception in the Human Medial Temporal Lobe

Thomas P. Reber,^{1,4} Jennifer Faber,^{1,2,4} Johannes Niediek,¹ Jan Boström,³ Christian E. Elger,¹ and Florian Mormann^{1,5,*}

¹Department of Epileptology, University of Bonn Medical Center, Sigmund-Freud-Str. 25, 53105 Bonn, Germany

²Department of Neurology, University of Bonn Medical Center, Sigmund-Freud-Str. 25, 53105 Bonn, Germany

³Department of Neurosurgery, University of Bonn Medical Center, Sigmund-Freud-Str. 25, 53105 Bonn, Germany

⁴These authors contributed equally

⁵Lead Contact

*Correspondence: florian.mormann@ukbonn.de

<http://dx.doi.org/10.1016/j.cub.2017.08.025>

SUMMARY

The neuronal mechanisms giving rise to conscious perception remain largely elusive [1]. It is known that the strength of single-neuron activity correlates with conscious perception, especially in anterior regions of the ventral pathway in non-human primates [2–4] and in the human medial temporal lobe (MTL) [5, 6]. It is unclear, however, whether single-neuron correlates of conscious perception are characterized solely by the magnitude of neuronal responses, and whether the correlates of perception are equally prominent across different regions of the human MTL. While recording from 2,735 neurons in 21 neurosurgical patients during 40 experimental sessions, we created experimental conditions in which otherwise identical visual stimuli are sometimes seen and sometimes not detected at all by means of the attentional blink, i.e., the phenomenon that the second of two target stimuli in close succession often goes unnoticed to conscious perception [7]. Remarkably, responses to unseen versus seen stimuli were delayed and temporally more dispersed, in addition to being attenuated in firing rate. This finding suggests precise timing of neuronal responses as a novel candidate physiological marker of conscious perception. In addition, we found modulation of neuronal response timing and strength in response to seen versus unseen stimuli to increase along an anatomical gradient from the posterior to the anterior MTL. Our results thus map out the neuronal correlates of conscious perception in the human MTL both in time and in space.

RESULTS

Attentional Blink Effectively Hides Stimuli from Awareness

During each trial of the attentional blink experiment, subjects were instructed to focus on two target images (T1/T2) that appeared in a subsequent stream of rapid serial visual presentation of images.

Subjects then reported separately for T1 and T2 whether they had seen it (Figure 1A; STAR Methods). Our analyses focus on the contrasts of trials in which the participant reported having seen the second target stimulus in the sequence or not (henceforth abbreviated by the terms “T2 seen” and “T2 unseen”). We observed less frequent “seen” reports for T2 than T1 images, especially at shorter lags between T1 and T2 (Figure 1B). Accordingly, a 2 × 4 repeated-measures ANOVA for 21 subjects with factors target (T1, T2) and lag (0 to 3 intermediary stimuli) on the percentage of seen responses revealed a significant interaction of lag × target ($F_{3,60} = 13.313$, $p = 9.120 \times 10^{-7}$, $\eta_p^2 = 0.400$). The main effects of target ($F_{1,20} = 27.145$, $p = 4.249 \times 10^{-5}$, $\eta_p^2 = 0.578$) and lag were likewise significant ($F_{3,60} = 7.962$, $p = 1.493 \times 10^{-4}$, $\eta_p^2 = 0.285$; see Tables S1 and S2 for post hoc comparisons). These results confirm that attentional blink creates a situation in which otherwise identical stimuli are sometimes consciously perceived and sometimes not detected at all.

Besides these classic attentional blink effects, we also found that the percentage of seen reports decreased with increasing number of intervening distractor stimuli between T2 and the response screen (5 intervening items: 86% seen, 6: 80%, 7: 79%, 8: 75%, 9: 73%, 10: 73%; repeated-measures one-way ANOVA: $F_{5,20} = 9.81$, $p = 1.19 \times 10^{-7}$, $\eta_p^2 = 0.329$). However, this effect cannot be properly isolated from the effect of lag as these factors are highly correlated ($R = .81$, $p < 0.001$). Furthermore, the percentage of false positive responses, i.e., responding with “seen” on catch trials in which the target stimulus was omitted, was low (median [Mdn] = 6.51%, interquartile range [IQR] = 11.46%), suggesting that only few misclassifications of awareness occurred.

Firing Rate and Response Latency of Single Neurons Correlate with Awareness

Action potentials from single neurons were recorded via microwires protruding from the shaft of electrodes implanted for epilepsy monitoring. Bilateral recording sites included amygdala (AM), hippocampus (HC), entorhinal cortex (EC), and parahippocampal cortex (PHC; see STAR Methods). The following analyses focus on a subset of 79 neurons that responded with increased firing selectively to only one of the stimuli and whose preferred stimulus was reported as unseen at least 4 times when presented as T2 (see STAR Methods).

In agreement with previous findings [5], some neurons responded in an all-or-none fashion to seen versus unseen

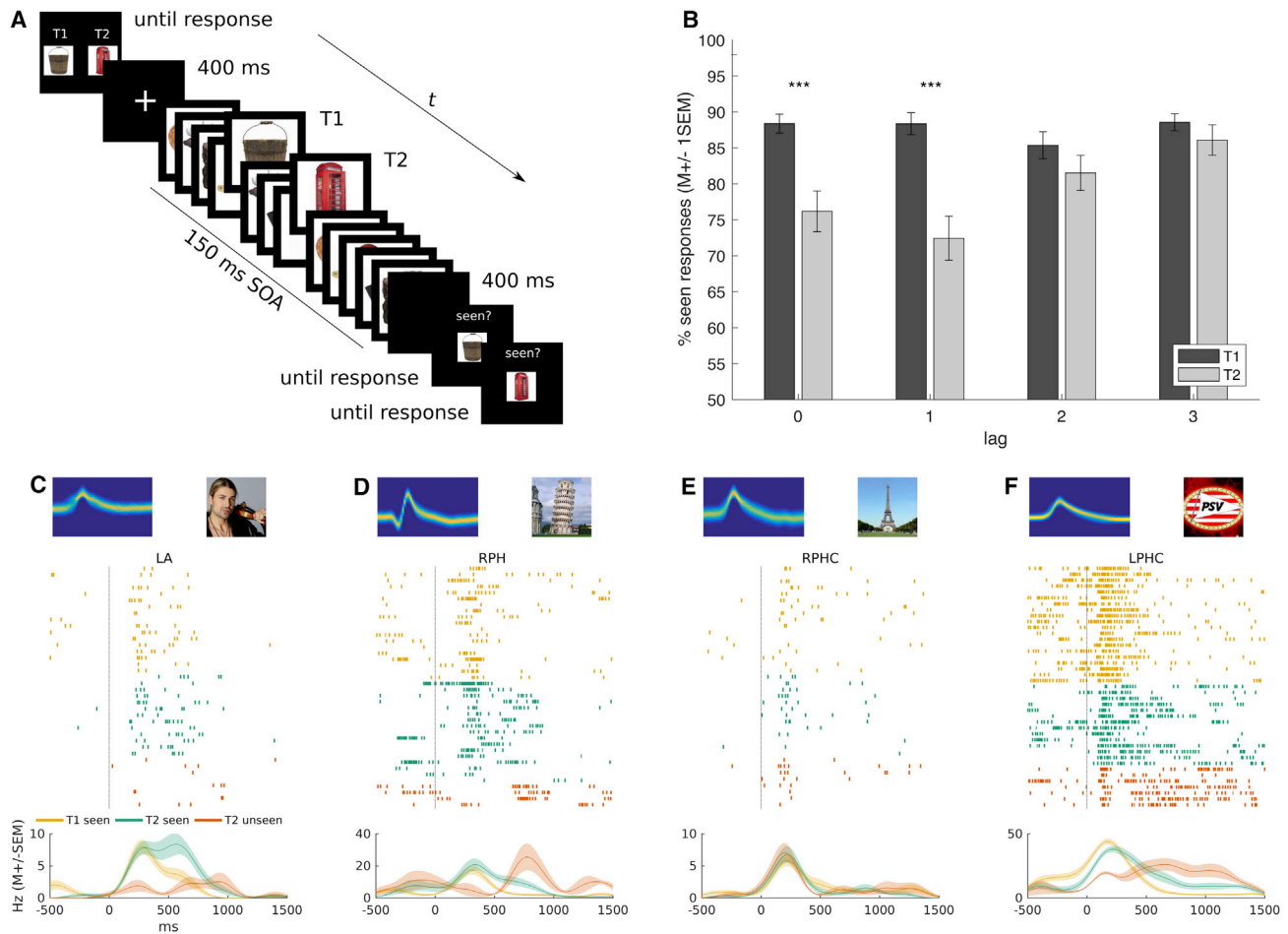


Figure 1. Experimental Paradigm and Examples of Single-Neuron Responses

(A) Sequence of events in one trial is shown from top left to bottom right. Eight stimuli presumed to elicit selective responses in individual neurons were selected in a preceding screening session (STAR Methods). During the main experiment, these eight stimuli were presented in a rapid serial visual presentation (RSVP) sequence. Participants were instructed to look out for two of these eight stimuli before the RSVP commenced. We use the term “T1” to designate the target stimulus that appears first in the sequence of rapid presentations and “T2” for the target stimulus that appears second. In any given trial, T1 and T2 were always two different images, except for catch trials in which either T2 or both target stimuli were omitted (see STAR Methods). The lag between T1 and T2 images varied from 0 to 3 (3 in the trial shown). The stimulus onset asynchrony (SOA) was usually 150 ms. After the RSVP stream, participants responded by button press whether or not they had seen T1 and T2, resulting in a classification of trials into T2 seen and T2 unseen.

(B) Behavioral results indicate that T2 versus T1 images were reported less often to have appeared in the sequence, which is indicative of attentional blink. See also Tables S1 and S2.

(C–F) Examples of single-neuron responses. The image in the top right of each panel depicts the stimulus that elicited a selective response for a neuron. A density plot of all spike waveforms is displayed in the top left. Raster plots depict observed spike times relative to stimulus onset of T1/T2 within the rapid presentation stream, color-coded per condition (yellow: T1 seen, green: T2 seen, red: T2 unseen). The graph below the raster plots shows mean instantaneous firing rates (Hz). Zero on the x axes denotes stimulus onset. RPH, right posterior hippocampus; LA, left amygdala; RPHC, right parahippocampal cortex; LPHC, left parahippocampal cortex.

presentations of the preferred stimulus (Figure 1C). Activity in other neurons, however, was delayed and temporally more dispersed, indistinguishable, or diminished for unseen versus seen trials (Figures 1D–1F, respectively).

Neurons Show a Gradient of Increasing Awareness-Related Response Activity from Posterior to Anterior MTL Regions

We computed the grand mean of normalized instantaneous firing rates (see STAR Methods) in medial temporal lobe (MTL) regions

and grouped responses into an anterior (AM, $n = 18$), intermediate (HC/EC, $n = 26$), and posterior (PHC, $n = 35$) region. Awareness-related activity was computed as the difference between normalized instantaneous firing following the preferred stimulus presented as T2 seen and T2 unseen (Figure 2E). As omnibus test, we used a cluster-based permutation test based on a one-way ANOVA (see STAR Methods) with the factor anatomical region (AM, HC/EC, PHC). Activity difference was smallest in PHC, intermediate in HC/EC, and largest in AM in a cluster ranging from 308 to 553 ms post-stimulus ($p = 0.003$; Figure 2F;

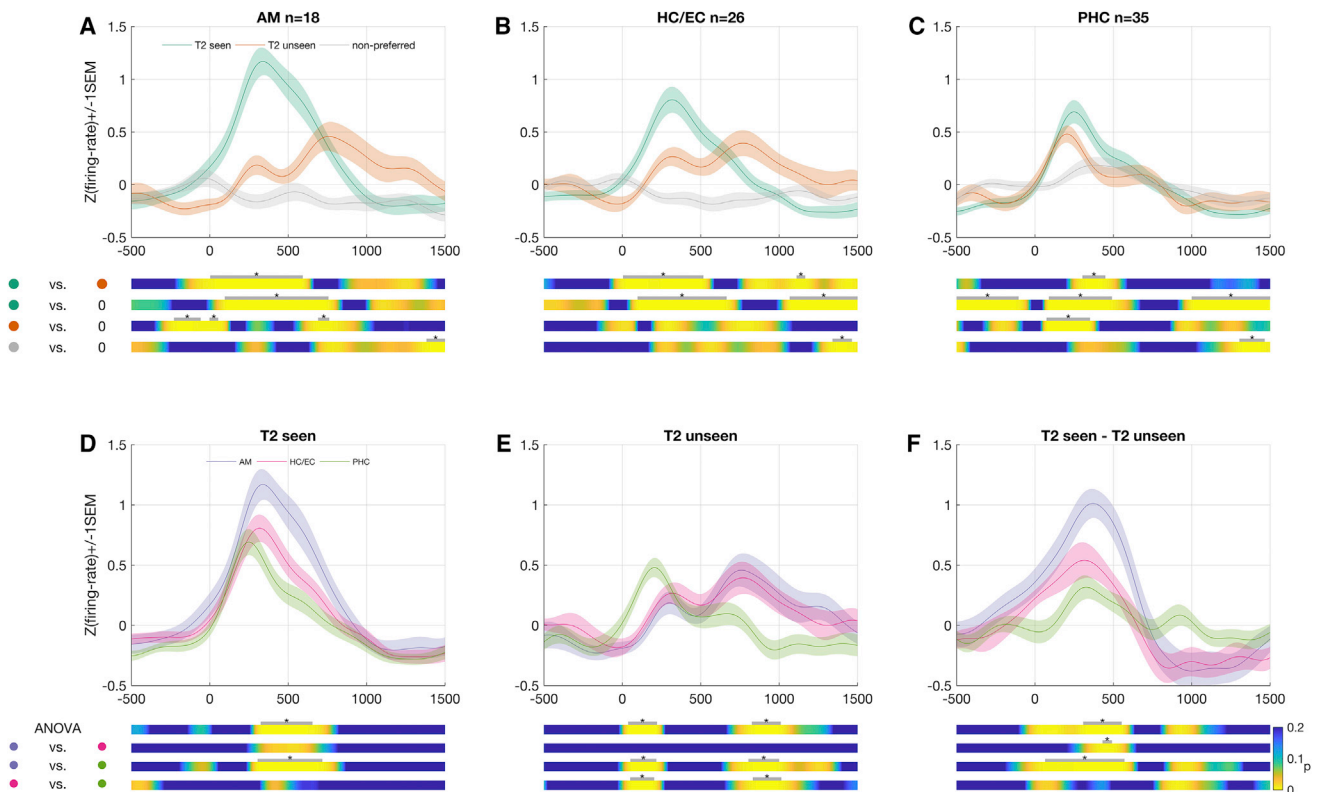


Figure 2. Awareness-Related Response Activity Increases from Posterior to Anterior MTL Regions

(A–C) Z-score-normalized instantaneous firing rates (STAR Methods) were first averaged across T2 seen and T2 unseen trials and then averaged across neurons in amygdala (AM; A), hippocampus/entorhinal cortex (HC/EC; B), and parahippocampal cortex (PHC; C). Green and red curves depict average responses to preferred stimuli presented as T2 seen and unseen, respectively. Gray curves depict average responses to the non-preferred stimuli with the lowest p value of the response criterion (second-most-preferred stimulus; STAR Methods) presented as T2 seen (see Figure S1 for responses to all non-preferred stimuli). Colored bars display p values of paired-samples t tests for T2 seen versus T2 unseen conditions and one-sample t test of individual curves against 0. (D–F) Comparisons across anatomical regions of T2 seen (D) and T2 unseen (E) and of the difference between these two conditions (F). Colored bars below the plots represent p values of a one-way ANOVA with factor region (AM, HC/EC, PHC) and p values from paired-samples t tests between regions. A gray line with an asterisk above the colored bars indicates a significant cluster ($p < 0.05$) resulting from a label-shuffling test (STAR Methods; Table S3). Standard errors of the mean (SEMs) were computed by taking the standard deviation (SD) of 400 bootstraps of the mean.

see Table S3 for significant clusters and pairwise comparisons). This effect was mainly driven by differences in firing strength to seen targets across regions (Figure 2D; Table S3), while firing to unseen targets was similar in strength (but not in latency; see below) across regions (Figure 2E; Table S3). Comparisons of instantaneous firing to seen versus unseen stimuli for individual anatomical regions corroborated these findings (Figures 2A–2C; Table S3). Neurons fired selectively to only one of the stimuli, and firing in response to non-preferred stimuli did not exceed baseline (Figures 2A–2C and S1).

Neurons throughout the MTL Respond to their Preferred Stimulus Even when It Is Reported as Unseen

We computed receiver operating characteristics (ROC) and corresponding areas under the curve (AUC), treating spikes following the preferred versus non-preferred stimulus as true versus false positives, respectively. ROCs were computed in moving windows of 200 ms width in 1 ms steps (Figures 3A and 3D; Table S4). Significant above-chance classification of the presence or absence of the preferred stimulus was possible throughout the

MTL, even when the stimulus was reported as unseen (AUC > 0.5; cluster permutation test; STAR Methods; Figures 3B and 3E).

While the peak amplitudes of AUC profiles of T2 unseen trials were similar across regions, their peak latency varied (Figure 3E; Table S4). Stimulus identity could be distinguished earlier in posterior (AUC > 0.5, PHC: 95–302 ms, $p < 0.001$) than in intermediate and anterior (AUC > 0.5, HC/EC: 205–222 ms, $p = 0.015$ and 224–341 ms, $p = 0.002$; AM: 227–274 ms, $p = 0.002$) neurons. Intermediate and anterior activity could be used to decode stimulus identity even at later time periods (Figure 3; Table S4).

Neuronal Firing in Anterior MTL Regions Predicts Awareness

We calculated moving window ROC analyses treating T2 seen versus T2 unseen activity following presentation of the preferred stimulus as true versus false positives, respectively (Figure 3C). Anatomical regions differed in whether reported awareness could be reliably decoded (cluster permutation ANOVA: 384–438 ms, $p = 0.012$). Neuronal activity in anterior and intermediate MTL regions reliably distinguished T2 seen versus T2 unseen in

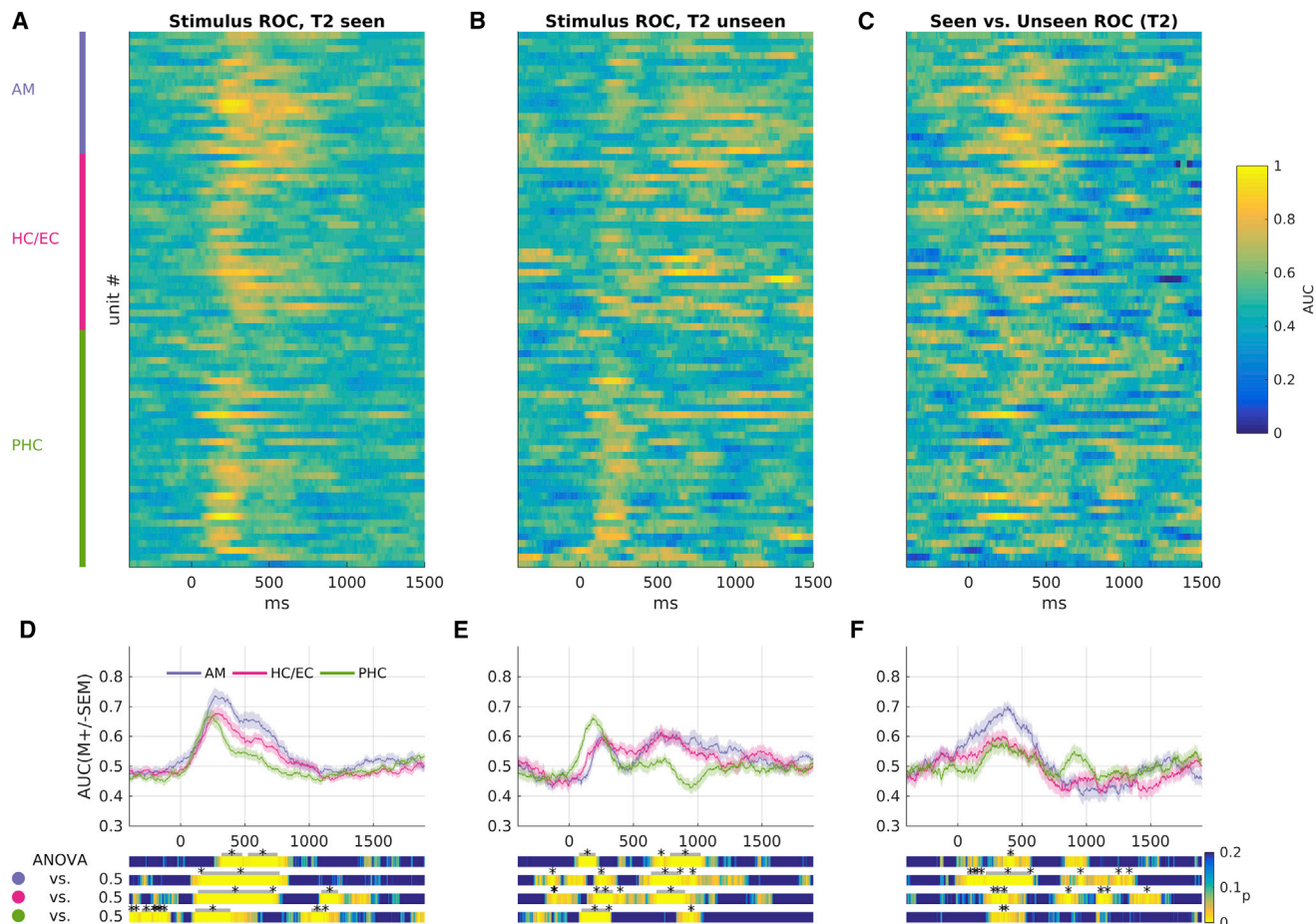


Figure 3. Neuronal Signals in Response to Unseen Stimuli Are Found Even in Anterior Regions of the MTL

(A–F) Receiver operating characteristics (ROCs) were computed for the classification of the stimulus identity following the T2 seen (A and D) and T2 unseen (B and E) and the classification of whether the stimulus was later reported as seen or not (C and F). ROCs were computed in sliding windows of 200 ms width in 1 ms steps. The resulting area under the curve (AUC) is depicted color-coded for every responsive cell ($n = 79$; A–C) and as average per anatomical region (D–F; AM, HC/EC, PHC). Color bars at the bottom depict p values of a one-way ANOVA with the factor region and of a one-sample t test against 0.5 for each individual curve. Significant clusters are marked by gray lines with an asterisk and result from label-shuffling tests ($p < 0.05$; STAR Methods; Table S4). SEMs were computed by taking the SD of 400 bootstraps of the mean.

multiple clusters between 73 and 569 ms (Table S3). In posterior regions (PHC), in contrast, only two small clusters reached significance (PHC, $AUC > 0.5$: 342–350 ms, $p = 0.035$, 371–377 ms, $p = 0.037$).

Neuronal Responses to Unseen versus Seen Stimuli Are Delayed and Temporally Dispersed

ROC analyses (Figure 3) and analyses of instantaneous firing rates (Figure 2) suggest that the latency of neuronal responses in anterior MTL regions indicates awareness. As both methods have rather limited temporal resolution (due to kernel convolution, moving windows), we next conducted a Poisson burst detection analysis to estimate neuronal response latencies [8, 9] (see STAR Methods). Response latencies for T2 unseen stimuli differed significantly across anatomical regions (AM, HC/EC, PHC; Figure 4E; $H = 8.80$, $p = 0.012$, Kruskal-Wallis test). Pairwise comparisons by Mann-Whitney U tests indicated that latencies of AM neurons (Mdn = 430 ms, IQR = 321 ms) were

longer than those of PHC neurons (Mdn = 330 ms, IQR = 194 ms; $p = 0.007$). Similarly, latencies in HC/EC (Mdn = 414 ms, IQR = 164 ms) were longer than in PHC (Mdn = 330 ms, IQR = 194 ms; $p = 0.043$). Latencies in AM (Mdn = 430 ms, IQR = 321 ms) were similar to those in HC/EC (Mdn = 414 ms, IQR = 164 ms; $p = 0.290$).

Longer latencies in HC/EC and AM neurons were specific to unseen trials as T2 seen latencies did not differ across anatomical regions (Figure 4D; $H = 1.380$, $p = 0.502$, Kruskal-Wallis test). We also calculated the difference between T2 seen and T2 unseen latencies per neuron. Again, anatomical regions differed significantly (Figure 4E; $H = 6.06$, $p = 0.048$, Kruskal-Wallis test). Post hoc Mann-Whitney U tests indicated that this was mainly due to stronger slowing of T2 unseen versus T2 seen responses in AM (Mdn = –214 ms, IQR = 246 ms) than PHC (Mdn = 9 ms, IQR = 171 ms; $p = 0.020$).

Neuronal response latencies to distractor stimuli during the RSVP sequence did not differ significantly across anatomical

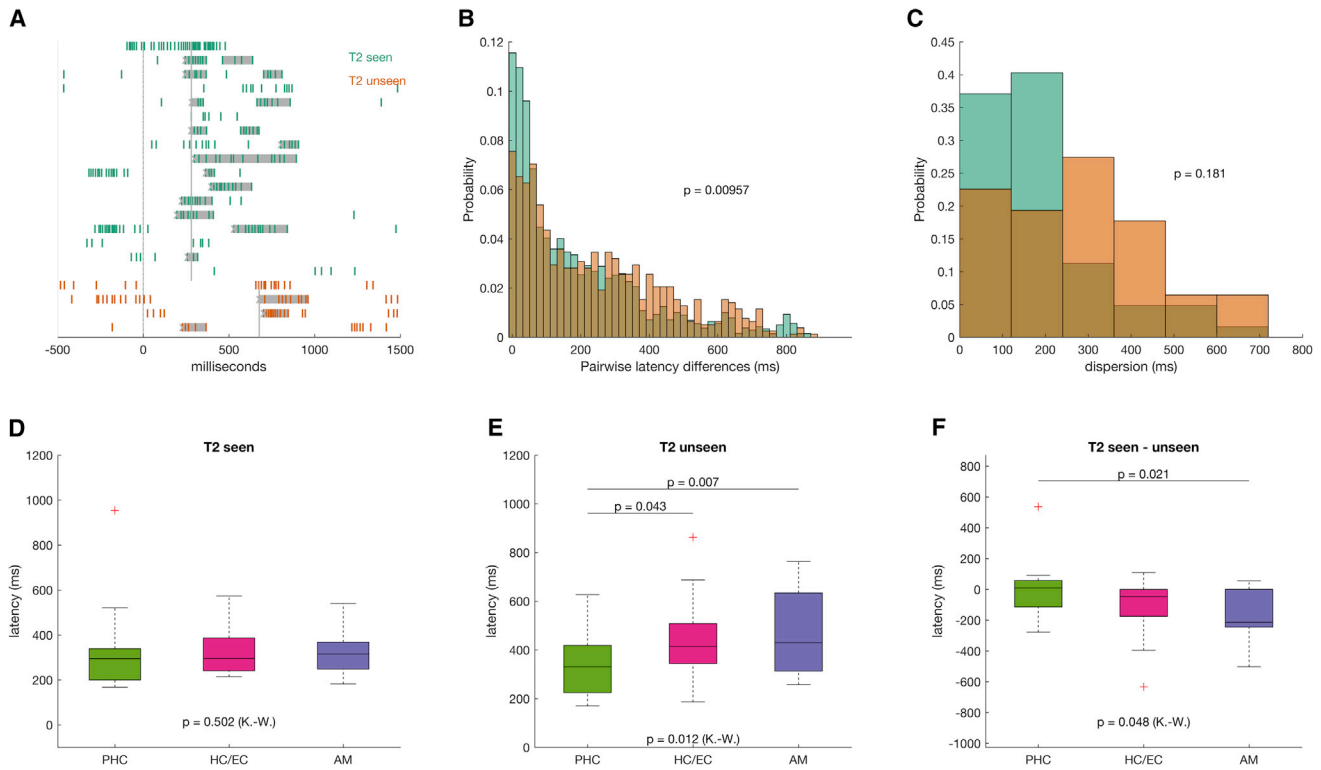


Figure 4. Neuronal Responses to Unseen versus Seen Targets Are Delayed and Temporally More Dispersed

(A) Latency of neuronal responses were estimated using a Poisson-burst detection algorithm. Gray areas mark bursts; gray vertical lines denote the medians of burst onsets across T2 seen and T2 unseen trials, respectively, which were taken as estimates of latency of neuronal firing (see also Figure S4).

(B and C) Normalized histograms of dispersion of latencies for seen and unseen targets across all regions.

(B) Differences between pairs of trialwise latency values computed for each condition and each neuron (STAR Methods).

(C) Histograms of the 2/3 of latency values closest to the median for each neuron and condition (seen versus unseen; STAR Methods).

(D–F) Boxplots denote response latencies for each anatomical region. p values beneath the boxes result from a Kruskal-Wallis test (K-W.) comparing anatomical regions, and p values above the boxes result from pairwise comparisons between regions using the Wilcoxon rank-sum test.

See also Figure S2 for correlations between measures of response latency and magnitude and Figure S3 for response latencies to distractors and response screen presentations.

regions. In contrast, neuronal response latencies for stimuli presented during the response screen were found to be earlier in PHC than AM and HC/EC as previously reported [9] (Figure S3).

To investigate effects on response latencies more closely (see also Figure S4), we assessed the dispersion of latency values using two separate measures. First, we calculated the pairwise differences between trialwise response latencies. Second, we calculated the range of the 2/3 of values closest to the median (see STAR Methods). Pairwise latency differences were larger for T2 unseen than T2 seen overall ($p = 9.57 \times 10^{-3}$, Brown-Forsythe test [10] with bootstrapping; see STAR Methods; Figure 4B), which was mainly driven by neurons in the amygdala (AM $p = 7.66 \times 10^{-7}$, HC/EC $p = 0.350$, PHC $p = 0.273$). Distributions of latency ranges for T2 seen and unseen revealed a similar pattern, but the difference in dispersion did not reach significance (overall $p = 0.181$; Figure 4C). Note that response latency and dispersion were independent from measures of response magnitude (Figure S2). Finally, in the 37 cells for which burst lengths could be determined (STAR Methods), no significant difference in burst length between T2 seen and T2 unseen trials could be observed (Wilcoxon signed-rank test, $p = 0.519$).

DISCUSSION

Our results show that not only strength but also the latency of MTL neuronal firing correlates with conscious perception. Thus, we propose stereotypical and precise timing of neuronal spiking activity as a novel candidate correlate of consciousness in humans. Furthermore, our study reveals an anatomical gradient along which neuronal activity is increasingly modulated in response to consciously versus unconsciously perceived visual stimuli. While neuronal responses in posterior MTL neurons were similar for seen and unseen targets, responses in intermediate and particularly anterior regions occurred later, were temporally more dispersed, and were attenuated for unseen versus seen targets. Neuronal activity following unseen stimulus presentations was nevertheless present throughout the MTL such that we could decode the presence or absence of the preferred stimuli.

In line with our findings, highly stereotypical response latencies have been observed in monkey and rodent sensory areas, and the timing of the response to a stimulus was found to carry as much or even more information than a rate code

that integrates firing over hundreds of milliseconds [11–13]. Together with slow oscillatory network activity in lower frequency ranges (2–6 Hz) [14], precise and stereotypical neural response latencies have been suggested to provide ensuing neural processes with a temporal reference frame for segmenting spiking activity into informative patterns. A failure of this segmentation may have caused the attentional blinks observed in our study since neuronal responses were delayed, and inter-trial variance of neuronal response latencies was increased for unseen versus seen stimuli. One could conjecture that delayed and more dispersed spiking reflects a failure of temporal selective attention—an idea put forward by recent scalp EEG and behavioral studies. In these studies, T1 and T2 were marked as targets by adding a circle around the stimulus (a letter) during the rapid presentation sequence, and participants were required to report the circled letters [15, 16]. Attentional blinks manifested in more frequent reports of the non-target stimulus following rather than preceding T2 [15, 16]. Furthermore, delayed and reduced P300 components have been observed following unseen versus seen targets in scalp EEG studies [17, 18]. Along these lines, mental training has been shown to increase target detection at the behavioral level and to yield temporally more consistent processing as indexed by increased inter-trial phase consistency in the theta range [19]. While the relationship between these low-frequency components and single-neuron activity is obviously complex [20], it is nevertheless remarkable that these three aspects of a failure of temporal selective attention observed in scalp EEG studies—namely reduced, delayed, and temporally more dispersed electrophysiological activity—can also be observed at the level of single neurons in the MTL.

Our data suggest that neurons throughout the MTL fire in response to their preferred stimuli even if subjects report unawareness of them. This finding suggests that neural events correlate with consciousness in a graded rather than an all-or-none fashion [21–23] and adds that significant information about the identity of the preferred stimulus can be read out from neural activity in the MTL, even when it is not consciously perceived. This finding contrasts with studies reporting absence of unit firing in the MTL in response to unseen stimuli. One study used brief presentations and backward masking [5]. Two other studies used binocular rivalry and flash suppression [6, 24], which entails the concurrent presentation of stimuli likely competing for resources within the visual processing stream. These procedures could plausibly block processing at earlier stages of the visual pathway outside the MTL. Neural signals following unseen trials during attentional blink, in contrast, have previously been reported to reach posterior MTL structures, albeit scalp EEG and fMRI were used in these studies [25–27]. For example, attentional blinks elicit event-related potential components associated with semantic processing that likely originate from MTL structures [17, 28–31] and elicit fMRI signals in posterior MTL regions [25]. Our single-unit data reveal that stimulus-specific neural signals can reach up to intermediate (HC/EC) and even anterior (AM) parts of the MTL. Although stimulus-specific information is available in unit firing throughout the MTL even though participants report unawareness of the stimuli, it is being discussed whether this information can become behaviorally relevant, e.g., in implicit MTL-dependent memory [32–34].

While attentional blink is an established paradigm to isolate neural correlates of consciousness (e.g., [17, 25, 35]), memory-related mechanisms may also play a role in whether a target is reported as seen or not. In line with this notion, we found that intervening distractors between T2 and reporting modulate the percentage of T2 seen reports. Also, stimulus-specific firing could result from trials with weak sensory experience that is reported as unseen due to high criterion for seen reports. This problem could be alleviated by using additional response options for partial awareness. However, it cannot account for our finding of graded neuronal responses because previous studies reporting all-or-none responses also used binary response options [21–23].

Our results demonstrate an anatomical gradient of increased modulation of neural activity in response to seen versus unseen stimuli along the posterior-anterior axis of the MTL. Although neuronal activity in early visual areas can be modulated by higher cognitive mechanisms such as context and attention [36], it has also been shown that neural signals in these early areas are not correlated with awareness [37, 38]. Remarkably, our data reveal that neurons in posterior MTL regions (PHC) behave quite similarly in that they fired in response to their preferred stimulus in similar magnitudes and latencies regardless of whether the stimulus was later reported as seen or not. This suggests that neuronal representations in the PHC are not accessible to conscious experience, which connects with the notion that the PHC is at the lower end of a processing hierarchy within MTL structures [9]. In contrast, effects of reported awareness on neuronal response timing and magnitude were evident in intermediate and even more so in anterior regions, suggesting a gradient of increased tuning to the contents of conscious experience within the MTL. Our findings thus agree with notions that the neural correlates of consciousness can be pinned down anatomically [1, 21, 39, 40] and add that especially the anterior regions of the MTL accurately reflect the contents of conscious experience.

In conclusion, our findings suggest precise timing of neuronal responses as a novel candidate physiological marker of conscious perception. In addition, we found modulation of neuronal response timing and strength in response to seen versus unseen stimuli to increase along an anatomical gradient from posterior to anterior MTL. Our results thus map out the neuronal correlates of conscious perception in the human MTL both in time and in space.

STAR★METHODS

Detailed methods are provided in the online version of this paper and include the following:

- [KEY RESOURCES TABLE](#)
- [CONTACT FOR REAGENT AND RESOURCE SHARING](#)
- [EXPERIMENTAL MODEL AND SUBJECT DETAILS](#)
- [METHOD DETAILS](#)
 - Electrophysiological Recordings
 - Attentional Blink Paradigm
- [QUANTIFICATION AND STATISTICAL ANALYSIS](#)
 - Identification of Responsive Neurons
 - Computation of Instantaneous Firing Rates
 - Cluster-Based Permutation Statistics

- Estimation of Response Latencies
- Dispersion of Response Latencies
- DATA AND SOFTWARE AVAILABILITY

SUPPLEMENTAL INFORMATION

Supplemental Information includes four figures and four tables and can be found with this article online at <http://dx.doi.org/10.1016/j.cub.2017.08.025>.

AUTHOR CONTRIBUTIONS

F.M. designed the study. J.B. and F.M. implanted the electrodes. J.F., F.M., J.N., and T.P.R. collected the data. T.P.R. and F.M. analyzed the data and wrote the paper. T.P.R., J.F., J.N., J.B., C.E.E., and F.M. discussed the results and commented on the manuscript.

ACKNOWLEDGMENTS

We thank all patients for their participation, B. Samimzad for assistance with the spike sorting, and C. Koch, I. Fried, H. Slagter, and J. Herring for discussion. This research was supported by the Volkswagen Foundation, the German Research Council (MO930/4-1, SFB1089), and the Swiss National Science Foundation (P300P1_161178, PBBEP1_146288).

Received: May 21, 2017

Revised: July 24, 2017

Accepted: August 11, 2017

Published: September 21, 2017

REFERENCES

1. Koch, C., Massimini, M., Boly, M., and Tononi, G. (2016). Neural correlates of consciousness: progress and problems. *Nat. Rev. Neurosci.* *17*, 307–321.
2. Sheinberg, D.L., and Logothetis, N.K. (1997). The role of temporal cortical areas in perceptual organization. *Proc. Natl. Acad. Sci. USA* *94*, 3408–3413.
3. Logothetis, N.K., and Schall, J.D. (1989). Neuronal correlates of subjective visual perception. *Science* *245*, 761–763.
4. Logothetis, N.K. (1998). Single units and conscious vision. *Philos. Trans. R. Soc. B Biol. Sci.* *353*, 1801–1818.
5. Quiroga, R.Q., Mukamel, R., Isham, E.A., Malach, R., and Fried, I. (2008). Human single-neuron responses at the threshold of conscious recognition. *Proc. Natl. Acad. Sci. USA* *105*, 3599–3604.
6. Kreiman, G., Fried, I., and Koch, C. (2002). Single-neuron correlates of subjective vision in the human medial temporal lobe. *Proc. Natl. Acad. Sci. USA* *99*, 8378–8383.
7. Raymond, J.E., Shapiro, K.L., and Arnell, K.M. (1992). Temporary suppression of visual processing in an RSVP task: an attentional blink? *J. Exp. Psychol. Hum. Percept. Perform.* *18*, 849–860.
8. Hanes, D.P., Thompson, K.G., and Schall, J.D. (1995). Relationship of presaccadic activity in frontal eye field and supplementary eye field to saccade initiation in macaque: Poisson spike train analysis. *Exp. Brain Res.* *103*, 85–96.
9. Mormann, F., Kornblith, S., Quiroga, R.Q., Kraskov, A., Cerf, M., Fried, I., and Koch, C. (2008). Latency and selectivity of single neurons indicate hierarchical processing in the human medial temporal lobe. *J. Neurosci.* *28*, 8865–8872.
10. Brown, M.B., and Forsythe, A.B. (1974). Robust tests for the equality of variances. *J. Am. Stat. Assoc.* *69*, 364–367.
11. VanRullen, R., Guyonneau, R., and Thorpe, S.J. (2005). Spike times make sense. *Trends Neurosci.* *28*, 1–4.
12. Brasselet, R., Panzeri, S., Logothetis, N.K., and Kayser, C. (2012). Neurons with stereotyped and rapid responses provide a reference frame for relative temporal coding in primate auditory cortex. *J. Neurosci.* *32*, 2998–3008.
13. Panzeri, S., Ince, R.A.A., Diamond, M.E., and Kayser, C. (2014). Reading spike timing without a clock: intrinsic decoding of spike trains. *Philos. Trans. R. Soc. Lond. B Biol. Sci.* *369*, 20120467.
14. Kayser, C., Ince, R.A.A., and Panzeri, S. (2012). Analysis of slow (theta) oscillations as a potential temporal reference frame for information coding in sensory cortices. *PLoS Comput. Biol.* *8*, e1002717.
15. Vul, E., Hanus, D., and Kanwisher, N. (2008). Delay of selective attention during the attentional blink. *Vision Res.* *48*, 1902–1909.
16. Vul, E., Nieuwenstein, M., and Kanwisher, N. (2008). Temporal selection is suppressed, delayed, and diffused during the attentional blink. *Psychol. Sci.* *19*, 55–61.
17. Vogel, E.K., Luck, S.J., and Shapiro, K.L. (1998). Electrophysiological evidence for a postperceptual locus of suppression during the attentional blink. *J. Exp. Psychol. Hum. Percept. Perform.* *24*, 1656–1674.
18. Sessa, P., Luria, R., Verleger, R., and Dell'Acqua, R. (2007). P3 latency shifts in the attentional blink: further evidence for second target processing postponement. *Brain Res.* *1137*, 131–139.
19. Slagter, H.A., Lutz, A., Greischar, L.L., Nieuwenhuis, S., and Davidson, R.J. (2009). Theta phase synchrony and conscious target perception: impact of intensive mental training. *J. Cogn. Neurosci.* *21*, 1536–1549.
20. Voytek, B., and Knight, R.T. (2015). Dynamic network communication as a unifying neural basis for cognition, development, aging, and disease. *Biol. Psychiatry* *77*, 1089–1097.
21. Dehaene, S., Charles, L., King, J.-R., and Marti, S. (2014). Toward a computational theory of conscious processing. *Curr. Opin. Neurobiol.* *25*, 76–84.
22. Kanwisher, N. (2001). Neural events and perceptual awareness. *Cognition* *79*, 89–113.
23. Rees, G., Kreiman, G., and Koch, C. (2002). Neural correlates of consciousness in humans. *Nat. Rev. Neurosci.* *3*, 261–270.
24. Kreiman, G., Fried, I., and Koch, C. (2001). Single neuron responses in humans during binocular rivalry and flash suppression. *J. Vis.* *1*, 131.
25. Marois, R., Yi, D.-J., and Chun, M.M. (2004). The neural fate of consciously perceived and missed events in the attentional blink. *Neuron* *41*, 465–472.
26. Moutoussis, K., and Zeki, S. (2002). The relationship between cortical activation and perception investigated with invisible stimuli. *Proc. Natl. Acad. Sci. USA* *99*, 9527–9532.
27. Slagter, H.A., Johnstone, T., Beets, I.A.M., and Davidson, R.J. (2010). Neural competition for conscious representation across time: an fMRI study. *PLoS ONE* *5*, e10556.
28. Elger, C.E., Grunwald, T., Lehnertz, K., Kutas, M., Helmstaedter, C., Brockhaus, A., Van Roost, D., and Heinze, H.J. (1997). Human temporal lobe potentials in verbal learning and memory processes. *Neuropsychologia* *35*, 657–667.
29. Geukes, S., Huster, R.J., Wollbrink, A., Junghöfer, M., Zwitserlood, P., and Döbel, C. (2013). A large N400 but no BOLD effect—comparing source activations of semantic priming in simultaneous EEG-fMRI. *PLoS ONE* *8*, e84029.
30. Guillem, F., N'Kaoua, B., Rougier, A., and Claverie, B. (1995). Intracranial topography of event-related potentials (N400/P600) elicited during a continuous recognition memory task. *Psychophysiology* *32*, 382–392.
31. Luck, S.J., Vogel, E.K., and Shapiro, K.L. (1996). Word meanings can be accessed but not reported during the attentional blink. *Nature* *383*, 616–618.
32. Greene, A.J. (2007). Human hippocampal-dependent tasks: is awareness necessary or sufficient? *Hippocampus* *17*, 429–433.
33. Henke, K. (2010). A model for memory systems based on processing modes rather than consciousness. *Nat. Rev. Neurosci.* *11*, 523–532.
34. Smith, C., and Squire, L.R. (2005). Declarative memory, awareness, and transitive inference. *J. Neurosci.* *25*, 10138–10146.

35. Sergent, C., Baillet, S., and Dehaene, S. (2005). Timing of the brain events underlying access to consciousness during the attentional blink. *Nat. Neurosci.* *8*, 1391–1400.
36. Self, M.W., Peters, J.C., Possel, J.K., Reithler, J., Goebel, R., Ris, P., Jeurissen, D., Reddy, L., Claus, S., Baayen, J.C., and Roelfsema, P.R. (2016). The effects of context and attention on spiking activity in human early visual cortex. *PLoS Biol.* *14*, e1002420.
37. Fisch, L., Privman, E., Ramot, M., Harel, M., Nir, Y., Kipervasser, S., Andelman, F., Neufeld, M.Y., Kramer, U., Fried, I., and Malach, R. (2009). Neural “ignition”: enhanced activation linked to perceptual awareness in human ventral stream visual cortex. *Neuron* *64*, 562–574.
38. Bacon-Macé, N., Macé, M.J.-M., Fabre-Thorpe, M., and Thorpe, S.J. (2005). The time course of visual processing: backward masking and natural scene categorisation. *Vision Res.* *45*, 1459–1469.
39. Baars, B.J. (1997). In the theatre of consciousness: global workspace theory, a rigorous scientific theory of consciousness. *J. Conscious. Stud.* *4*, 292–309.
40. Dehaene, S., and Changeux, J.-P. (2011). Experimental and theoretical approaches to conscious processing. *Neuron* *70*, 200–227.
41. Quiroga, R.Q., Nadasdy, Z., and Ben-Shaul, Y. (2004). Unsupervised spike detection and sorting with wavelets and superparamagnetic clustering. *Neural Comput.* *16*, 1661–1687.
42. Brainard, D.H. (1997). The psychophysics toolbox. *Spat. Vis.* *10*, 433–436.
43. Hentschke, H., and Stüttgen, M.C. (2011). Computation of measures of effect size for neuroscience data sets. *Eur. J. Neurosci.* *34*, 1887–1894.
44. Mormann, F., Dubois, J., Kornblith, S., Milosavljevic, M., Cerf, M., Ison, M., Tsuchiya, N., Kraskov, A., Quiroga, R.Q., Adolphs, R., et al. (2011). A category-specific response to animals in the right human amygdala. *Nat. Neurosci.* *14*, 1247–1249.
45. Simes, R.J. (1986). An improved Bonferroni procedure for multiple tests of significance. *Biometrika* *73*, 751–754.
46. Maris, E., and Oostenveld, R. (2007). Nonparametric statistical testing of EEG- and MEG-data. *J. Neurosci. Methods* *164*, 177–190.

STAR★METHODS

KEY RESOURCES TABLE

REAGENT or RESOURCE	SOURCE	IDENTIFIER
Software and Algorithms		
MATLAB	MathWorks	https://www.mathworks.com
Wave_clus	[41]	https://github.com/csn-le/wave_clus
Custom-built MATLAB code	This paper	N/A
Octave	GNU	https://www.gnu.org/software/octave/
Psychtoolbox	[42]	http://psychtoolbox.org/
Measures of effect size toolbox	[43]	https://sourceforge.net/projects/mestoolbox/

CONTACT FOR REAGENT AND RESOURCE SHARING

Further information and requests for resources should be directed to and will be fulfilled by the Lead Contact, Florian Mormann (florian.mormann@ukbonn.de).

EXPERIMENTAL MODEL AND SUBJECT DETAILS

Subjects were 21 epilepsy patients (12 male; age M [SD] = 37.86 [10.89] years) with MTL depth electrodes implanted for chronic seizure monitoring. The typical duration of EEG monitoring was seven to ten days, during which patients participated in various cognitive experiments. The study conformed to the guidelines of the Medical Institutional Review Board at the University of Bonn. Informed written consent was obtained from each subject.

METHOD DETAILS

Electrophysiological Recordings

Recordings were obtained from a bundle of nine microwires (eight high-impedance recording electrodes, one low-impedance reference, AdTech, Racine, WI) protruding from the end of each depth electrode. The differential signal from the microwires was amplified using a Neuralynx ATLAS system (Bozeman, MT), filtered between 0.1 and 9,000 Hz, and sampled at 32 kHz. These recordings were stored digitally for further analysis. Recording electrodes were either referenced against one of the reference electrodes or in a bipolar scheme, depending on signal quality. Spike detection, and sorting was performed after band-pass filtering the signals between 300 and 3,000 Hz as described previously [41, 44]. The number of recording microwires per patient ranged from 32 to 96.

Attentional Blink Paradigm

A standard laptop running the Psychophysics Toolbox (www.psychtoolbox.org/ [42]) under MATLAB (<https://www.mathworks.com>) was used for stimulus presentation. The refresh rate of the display was set to 60 Hz. The stimulus set for each experimental session consisted of eight stimuli that were selected based on the results of a preceding screening procedure as being likely to elicit selective responses in one or more of the recorded neurons [10, 11].

Participants were tested at bedside and instructed to report on each trial whether two target images (T1 and T2) were among a sequence of 14 images presented in rapid succession (Figure 1A). At the beginning of a trial, participants were prompted with a screen showing T1 and T2 side by side. After confirmation of the prompt by button press, a fixation cross was presented for 400 ms, then the rapid serial visual presentation of the 14 images commenced. Thereafter, a blank screen for 400 ms was followed by two separate queries if the participants had seen the target images (T1/T2) during the rapid presentation sequence or not (response screen).

Each session consisted of 216 trials and was split into three runs of 72 trials each. The sequence of trials was randomized within a run. Each of the eight response-eliciting images were chosen to be either T1 or T2 an equal number of times. Additionally, in 16 randomly selected trials per run, either only T2 (eight trials) or T1 and T2 (eight trials) were omitted during the rapid presentation sequence yielding slightly varying amounts of T1/T2 trials per image. These catch-trials were introduced to assess the false positive rate of seen reports. The position of T1 and T2 in the sequence was set pseudorandomly with the constraints that T1 position ranged from 3rd to 5th, the lag between T1 and T2 ranged between zero and three intervening image presentations. The remaining 12 positions in the rapid presentation sequence were pseudorandomly filled with the remaining six images, i.e., distractors, with the constraint that identical images were not presented successively. The default stimulus onset asynchrony (SOA) in the rapid presentation sequence was 150 ms (35 sessions), but was reduced to SOAs in the range of 100 to 135 ms in patients who reported only few unseen trials in their first session (five sessions).

QUANTIFICATION AND STATISTICAL ANALYSIS

Identification of Responsive Neurons

Spike counts were obtained in 19 overlapping 100-ms-bins in a response window ranging from 0 to 1,000 ms post stimulus, and during a baseline window ranging from -400 to 0 ms for each presentation of an image as distractor. A Wilcoxon signed-rank test treating trialwise baseline and response window spike counts as pairs was computed for each of the 19 bins. Spike counts were normalized to the corresponding bin size. Resulting p values were corrected for multiple comparison using the Simes procedure [45]. The lowest p value after correction was used to quantify the strength by which a unit responded with increased firing to a certain stimulus.

A p value threshold for considering a unit as responding to a stimulus was derived by the following. Raster plots of unit responses with a p value < 0.001 were visually inspected by four experienced electrophysiologists and rated as valid responses or not. Raters were generally in good agreement (Fleiss' $\kappa = 0.78$). Responses were considered "true" if at least two of the raters judged a raster plot as a valid response. The optimal p value threshold ($p < 5 \times 10^{-6}$) was derived from Receiver Operating Characteristics (ROC), i.e., was defined as the point on the ROC curve with minimal distance to the top-left corner $([0, 1])$.

Computation of Instantaneous Firing Rates

To compare neuronal firing in response to a stimulus across conditions of interest (T2 seen versus T2 unseen), we computed Z scores of instantaneous firing rates. Instantaneous firing was approximated by trialwise convolution of spike trains with a Gaussian kernel (100 ms full width half maximum). These signals were Z transformed using the mean and standard deviation across all target presentations (T1/2, seen/unseen) of the signal after convolution averaged over a baseline interval ranging from -500 ms to stimulus onset (0 ms). Normalized signals were then averaged per unit and condition of interest (T2 seen, T2 unseen).

Cluster-Based Permutation Statistics

The reported cluster-based label shuffling statistics were computed as described previously [46]. Briefly, a series of either one sample, independent samples, or paired samples t tests is computed at each time point. The sum of t -values is computed for each cluster of contiguous time points at which the t test yields $p < 0.005$ (cluster-alpha). Sum of t -values are obtained once using the original assignments of labels to the data, and 1000 times with random assignments of condition labels to the data, i.e., label-shuffling. The resulting p value reflects the percentile of the sum of t -values obtained using the original assignment of labels in the distribution of sums of t -values obtained with random labels. We applied the same procedure to compare signals between anatomical regions. Here, we computed one-way ANOVAs and the sum of F -values per cluster.

Estimation of Response Latencies

Latency of neuronal firing in response to the preferred stimulus was estimated for each trial in a response-period from 100 to 1,000 ms post stimulus. For units with a baseline firing rate above 2 Hz, we used a poisson burst detection algorithm (Figure 4) [8, 9]. For units with a lower baseline firing rate (< 2 Hz), the first spike time within the response period was taken as measure of response latency. The median of these response latencies across trials was taken for the T2 seen and T2 unseen conditions for each unit. For these analyses, units were included only if latency values could be determined for at least two trials per condition of interest (T2 seen, T2 unseen). Sixty-two out of the 79 selected units (see above) met this criterion.

Dispersion of Response Latencies

We calculated two different measures to assess the dispersion of latency values. First, the absolute differences between all possible pairs of trialwise latencies for each unit were calculated separately for seen and unseen trials (i.e., pairwise latency differences, Figure 4B). Second, we took the two thirds of latencies values closest to median in each unit and condition (T2 seen and T2 unseen), and calculated the difference between the highest and lowest value of these latencies (i.e., latency range, Figure 4C). As there were more trials for T2 seen versus T2 unseen, we drew randomly as many trials from the T2 seen set as there were trials available for T2 unseen in each unit, calculated the F -value resulting from the Brown-Forsythe test for equality of variance [10], and repeated this procedure 1,000 times. The reported p value results from the median of these 1,000 F -values. This randomization procedure was applied both to pairwise latency differences and latency range.

DATA AND SOFTWARE AVAILABILITY

Data and custom-built MATLAB code can be requested by email from the Lead Contact.

Current Biology, Volume 27

Supplemental Information

**Single-Neuron Correlates of Conscious Perception
in the Human Medial Temporal Lobe**

Thomas P. Reber, Jennifer Faber, Johannes Niediek, Jan Boström, Christian E. Elger, and Florian Mormann

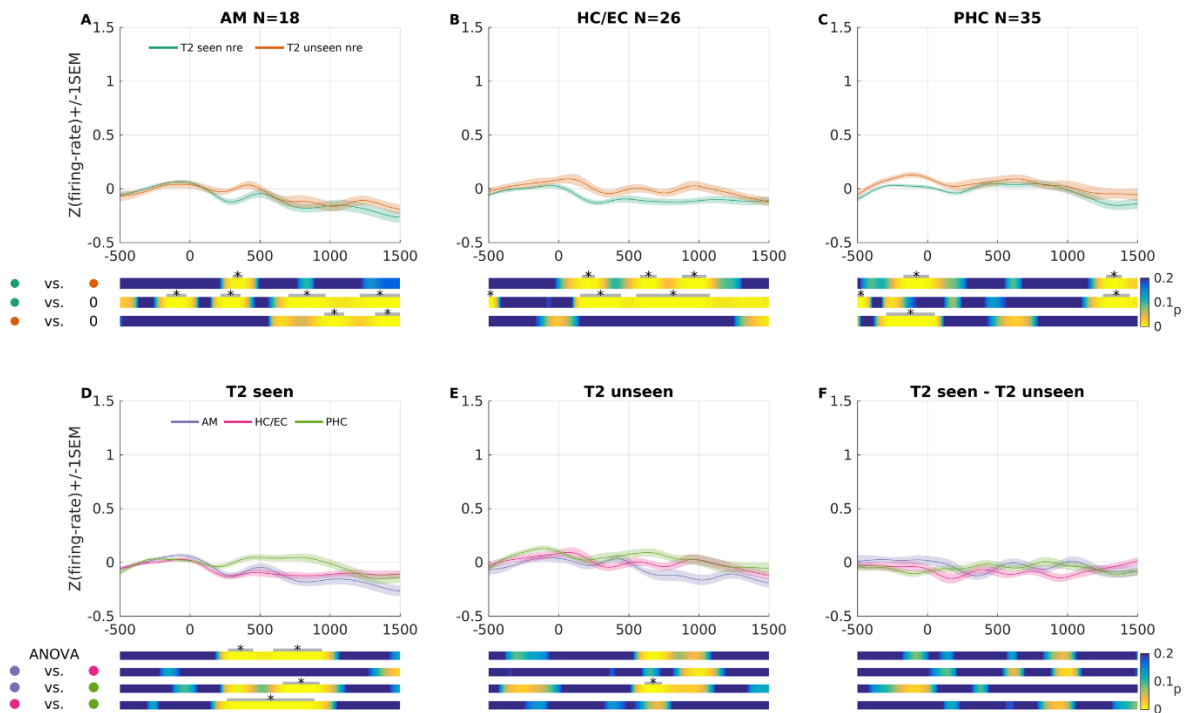


Figure S1, related to Figure 2. Awareness-related neuronal activity in response to non-preferred stimuli. Z-score-normalized instantaneous firing rates were first averaged across T2-seen and T2-unseen trials, and then averaged across neurons in Amygdala (AM, panel A), Hippocampus/ Entorhinal Cortex (HC/EC, panel B), and Parahippocampal Cortex (PHC, panel C). Green and red curves depict average response to preferred stimuli presented as T2 seen and unseen, respectively. Colored bars display p-values of paired-samples t-tests for T2-seen versus T2-unseen conditions, and one-sample t-test of individual curves against 0 (panels A-C). Panels D-F depict comparisons across anatomical regions of T2-seen (D), T2-unseen (E), and of the difference between these two conditions (F). Colored bars represent p-values of a one-way ANOVA with factor region (AM, HC/EC, PHC), and p-values from paired-samples t-tests between regions. A gray line with an asterisk above the colored bars indicates a significant cluster ($p < 0.05$) resulting from a label-shuffling test (see STAR Methods). Standard errors of the mean (SEM) were computed by taking the standard deviation (SD) of 400 bootstraps of the mean. nre, non-response-eliciting.

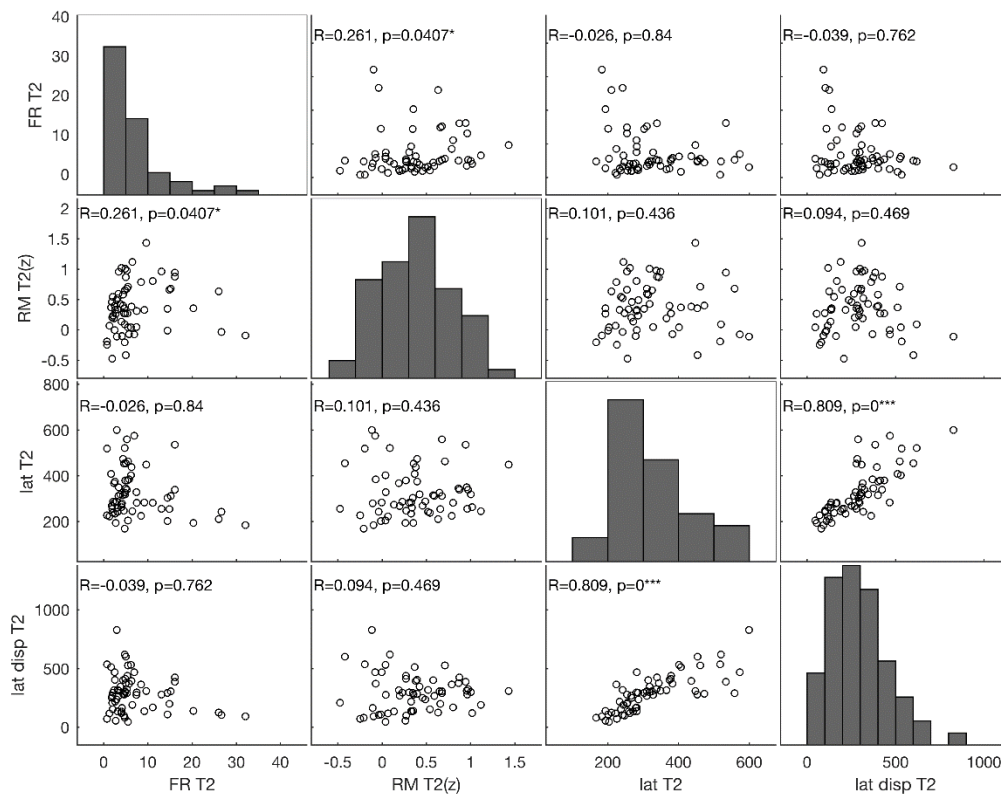


Figure S2, related to Figure 4. Correlation matrix of variables of response latency and magnitude. Spearman rank correlation matrix for variables calculated on spikes emitted following presentations of the preferred image as T2. RM: response magnitude, FR: firing rate, T2 s: T2-seen, lat: latency, disp: dispersion. Variables are the firing rate in Hz (“FR T2 s”) during the response window (0, 1000 ms), a z-score of the firing rate during the response window (“RM T2 s (z)”), the response latency (“lat T2 s”), median of trialwise latency values, see STAR Methods), and the dispersion of latency (“lat disp T2 s”, range of trialwise latency values, see STAR Methods). Z-scores were calculated by subtracting the firing rate during a response window (0 to 1000 ms post-stimulus) from the mean firing rate in a baseline-window (-500 to 0 ms) and dividing by the standard deviation of firing in the baseline window.

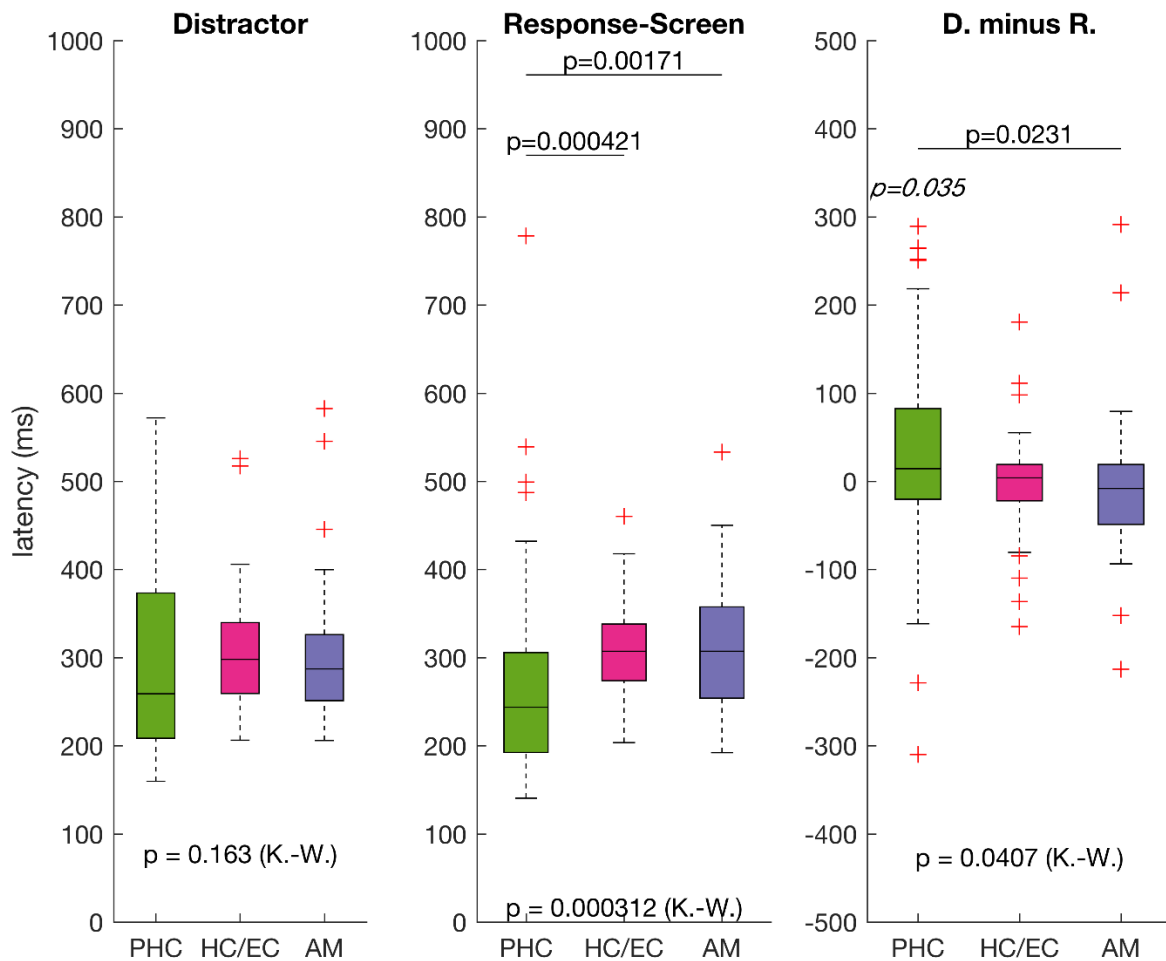


Figure S3, related to Figure 4: Response latencies to distractors and response screen presentations.

Neuronal response latencies following presentations of the preferred stimulus as distractor (left) and during the seen/unseen query (response-screen, middle), and pairwise differences between the two (distractor latency minus response-screen latency, i.e., D. minus R.). Note that the number of included cells for these analyses ($N=123$) is higher than for the analyses of T2 seen/unseen in the manuscript because we did not have to exclude cases in which stimuli were reported as unseen fewer than 4 times. P-values at the bottom are derived from Kruskal-Wallis test across anatomical regions. P-values of pairwise comparisons are indicated only if significant. P-values above horizontal lines are derived from Mann-Whitney U tests between anatomical regions, and the p-value in italics in the right plot is derived from a one-sample Wilcoxon signed-rank test against zero.

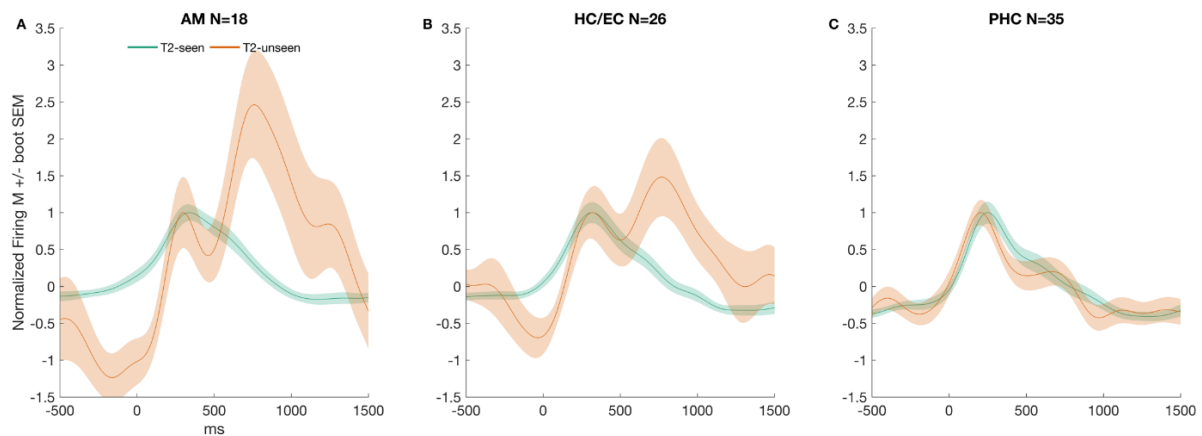


Figure S4, related to Figure 4: Curves of instantaneous firing normalized to their early maximum.

Curves of instantaneous firing were obtained as in Figure 2, and an additional step of normalization was performed: The curves were divided by their maximum in the time-window ranging from 0 to 500 ms post-stimulus (T2) to match peak firing amplitudes between seen and unseen. Note that the first of the two peaks of firing in response to unseen targets in AM and HC/EC seem to occur at a similar time as the peak of firing following seen targets. The latency difference we observe with analyses aimed at investigating response latency (Figure 4) thus seems to be reflected in both peaks of firing observed in response to unseen targets in Figure 2. Accordingly, we do not only find an increase in the median response latencies, but also an increase in the dispersion of single-trial response latencies in unseen trials. Figure 4A depicts a raster plot exemplifying how these two peaks of firing in response to unseen trials may come about. In one of four unseen trials, the cell bursts at a similar time as bursts occur during seen trials while bursts in the remaining three trials occur around the time of the second peak observed in the grand-averages of instantaneous firing (Figure 2). It appears that while in some trials and/or neurons there is no neuronal response latency effect, the frequency of delayed neuronal responses to unseen targets increases from posterior to anterior regions, resulting in increasingly prominent second peaks of instantaneous firing following T2 unseen stimuli from posterior to anterior regions.

Contrast	M ₁ (SD ₁)	M ₂ (SD ₂)	t(df)	p
Lag 0 vs. 1	76 (13)	72 (14)	1.29 (20)	0.211
Lag 0 vs. 2	76 (13)	82 (11)	-1.76 (20)	0.0934
Lag 0 vs. 3	76 (13)	86 (10)	-3.53 (20)	0.00208 *
Lag 1 vs. 2	72 (14)	82 (11)	-5.45 (20)	2.47×10 ⁻⁰⁵ *
Lag 1 vs. 3	72 (14)	86 (10)	-5.93 (20)	8.4×10 ⁻⁰⁶ *
Lag 2 vs. 3	82 (11)	86 (10)	-2.85 (20)	0.00988

* significant $p < 0.0083$ (0.05/6, Bonferroni corrected)

Table S1, related to Figure 1: Pairwise comparisons between lag levels on percent seen reports for T2.

	M _{T2} (SD _{T2})	M _{T1} (SD _{T1})	t(df)	p
Lag 0	76 (13)	88 (6)	-5.12 (20)	5.27×10 ⁻⁰⁵ *
Lag 1	72 (14)	82 (11)	-5.54 (20)	5.54×10 ⁻⁰⁵ *
Lag 2	82 (11)	85 (9)	-2.06 (20)	0.052
Lag 3	86 (10)	89 (5)	-1.43 (20)	0.168

* significant at $p < 0.0125$ (0.05/4, Bonferroni corrected)

Table S2, related to Figure 1: Pairwise comparisons of percent seen for T2 vs T1 for every lag level.

Figure	Contrast	from-to (ms)	p
Fig. 2A	AM: T2 seen > T2 unseen	3 to 593	<0.001
	AM: T2 seen > 0	96 to 757	<0.001
	AM: T2 unseen > 0	691 to 762	0.006
	AM: T2 unseen < 0	-228 to -58	0.004
	AM: T2 unseen < 0	-2 to 54	0.011
	AM: non-preferred < 0	1382 to 1500	0.005
Fig. 2B	HC/EC: T2 seen > T2 unseen	4 to 517	<0.001
	HC/EC: T2 seen < T2 unseen	1111 to 1166	0.017
	HC/EC: T2 seen > 0	97 to 665	<0.001
	HC/EC: T2 seen < 0	1067 to 1500	<0.001
	HC/EC: non-preferred < 0	1340 to 1464	<0.001
Fig. 2C	PHC: T2 seen > T2 unseen	303 to 449	0.002
	PHC: T2 seen > 0	89 to 491	<0.001
	PHC: T2 seen < 0	-500 to -104	<0.001
	PHC: T2 seen < 0	1000 to 1500	<0.001
	PHC: T2 unseen > 0	74 to 351	<0.001
Fig. 2D	PHC: non-preferred < 0	1304 to 1465	<0.001
	T2 seen: ANOVA	325 to 655	<0.001
Fig. 2E	AM > PHC	305 to 718	<0.001
	T2 unseen: ANOVA	37 to 221	0.004
Fig. 2F	T2 unseen: ANOVA	826 to 1010	0.019
	T2 unseen: AM > PHC	804 to 1000	0.004
	T2 unseen: AM < PHC	51 to 217	0.005
	T2 unseen: HC/EC > PHC	832 to 1014	0.008
	T2 unseen: HC/EC < PHC	50 to 203	0.006
	T2seen - unseen: ANOVA	308 to 553	0.003
Fig. 2F	T2seen - unseen: AM > HC/EC	431 to 491	0.031
	T2seen - unseen: AM > PHC	65 to 571	<0.001

Table S3, related to Figure 2: Significant clusters resulting from label shuffling tests of instantaneous firing in response to the preferred stimulus.

Figure	Contrast	from-to (ms)	p
Fig. 3A Stimulus ROC T2 seen	ANOVA	318 to 480	<0.001
	ANOVA	524 to 755	<0.001
	AM: AUC > 0.5	159 to 163	0.031
	AM: AUC > 0.5	164 to 771	<0.001
	HC/EC: AUC > 0.5	135 to 716	<0.001
	HC/EC: AUC > 0.5	717 to 724	0.032
	HC/EC: AUC < 0.5	1095 to 1226	<0.001
	PHC: AUC > 0.5	113 to 388	<0.001
	PHC: AUC < 0.5	-400 to -362	0.009
	PHC: AUC < 0.5	-355 to -337	0.018
	PHC: AUC < 0.5	-303 to -229	0.003
	PHC: AUC < 0.5	-210 to -203	0.040
	PHC: AUC < 0.5	-202 to -186	0.020
	PHC: AUC < 0.5	-174 to -167	0.042
	PHC: AUC < 0.5	-166 to -148	0.017
	PHC: AUC < 0.5	-145 to -107	0.010
	Fig. 3B Stimulus ROC T2 unseen	ANOVA	1018 to 1110
ANOVA		1120 to 1135	0.022
ANOVA		77 to 205	0.003
ANOVA		708 to 728	0.035
ANOVA		785 to 1024	<0.001
AM: AUC > 0.5		227 to 274	0.002
AM: AUC > 0.5		637 to 858	<0.001
AM: AUC > 0.5		861 to 870	0.025
AM: AUC > 0.5		947 to 980	0.009
AM: AUC < 0.5		-139 to -118	0.015
HC/EC: AUC > 0.5		205 to 222	0.015
HC/EC: AUC > 0.5		224 to 341	0.002
HC/EC: AUC > 0.5		394 to 399	0.043
HC/EC: AUC > 0.5		679 to 902	<0.001
HC/EC: AUC < 0.5		-123 to -117	0.028
HC/EC: AUC < 0.5		-116 to -109	0.026
Fig. 3C Seen vs. Unseen ROC (T2)		PHC: AUC > 0.5	95 to 302
	PHC: AUC > 0.5	304 to 316	0.032
	PHC: AUC < 0.5	938 to 962	0.019
	ANOVA	385 to 438	0.012
	AM: AUC > 0.5	73 to 124	0.003
	AM: AUC > 0.5	127 to 137	0.013
	AM: AUC > 0.5	138 to 162	0.006
	AM: AUC > 0.5	170 to 199	0.005
	AM: AUC > 0.5	217 to 562	<0.001
	AM: AUC > 0.5	564 to 569	0.027
	AM: AUC < 0.5	951 to 961	0.029
	AM: AUC < 0.5	1245 to 1259	0.017
	AM: AUC < 0.5	1333 to 1338	0.038
	HC/EC: AUC > 0.5	268 to 287	0.010
	HC/EC: AUC > 0.5	290 to 327	0.003
	HC/EC: AUC > 0.5	337 to 386	<0.001
	HC/EC: AUC < 0.5	845 to 879	0.006
HC/EC: AUC < 0.5	1093 to 1135	0.005	
HC/EC: AUC < 0.5	1157 to 1175	0.010	
HC/EC: AUC < 0.5	1470 to 1477	0.035	
PHC: AUC > 0.5	342 to 350	0.035	
PHC: AUC > 0.5	371 to 377	0.037	

Table S4, related to Figure 3: Significant clusters resulting from label shuffling tests of sliding window ROC.